Mol. Cryst. Liq. Cryst. 1994, Vol. 256, pp. 507–512
Reprints available directly from the publisher
Photocopying permitted by license only

THE EFFECT OF INTRINSIC RIGIDITY ON THE OPTICAL PROPERTIES OF PPV DERIVATIVES

C.L. GETTINGER and A.J. HEEGER
University of California, Santa Barbara Santa Barbara, California 93106
J.M. DRAKE and D.J. PINE
Exxon Research and Engineering Company Route 22 East,
Annandale, New Jersey 08801

Abstract Light scattering and optical spectroscopy experiments were performed on [2-methoxy, 5-(2'-ethyl-hexyloxy-p-phenylene-vinylene] (MEH-PPV), poly[2-butoxy, 5-(2'-ethyl-hexyloxy-p-phenylene-vinylene] (BEH-PPV), and poly[2-dicholestanoxy-p-phenylene-vinylene] (BCHA-PPV) in solution with p-xylene to determine the effects of side chain size on the structure and optical properties of PPV. We find that increasing the size of the solubilizing side chains increases the intrinsic persistence length of the PPV backbone and this change in rigidity has dramatic effects on the photoluminescence of PPV. Quantum yield determination relative to Rhodamine 6G shows the luminescence efficiency of the rigid BCHA-PPV is 0.66 ± 0.05 and that the yield decreases to 0.20 ± 0.05 for MEH-PPV, the most coiled derivative. Excitation profiles show an increase in non-radiative decay at high energies when the backbone is more flexible.

INTRODUCTION

There is currently much interest in PPV because of its application in luminescent devices[1-3]. Like many conjugated polymers, PPV is insoluble in its pure form due to a high dielectric mismatch with conventional solvents. This intractability has been addressed by chemically attaching side chains to the polymer backbone. Side chains provide an organic layer that surrounds the polymer backbone, much like a surfactant, and make the polymer more compatible with organic solvents. While many conjugated polymers are processed in the derivatized form, very little is understood about the effects of functionalization on the structural, optical, and electronic properties of these polymers. Both experimental and theoretical studies have shown that the steric interactions of the side chains induce significant rigidity of the polymer backbone[4,5].

The effect of macroscopic disorder on the optical properties of PPV and PPV derivatives have been studied extensively[6-9]. With techniques such as tensile drawing and gel processing, these experiments have shown that increased orientation and improved structural order produces a narrowing of both the absorption and emission spectra along with a reduction in apparent Stokes shift. These results have been interpreted as an increase in effective conjugation length, L_{eff} as a result of increased chain order. Still to be understood is how the effective conjugation length is derived from intrinsic polymer features.

In this paper we report a comparative study of the photoluminescence properties of three PPV derivatives: MEH-PPV, BEH-PPV, and BCHA-PPV (figure 1). Each has been derivatized with an increasingly larger side group in order to solubilize the PPV. With static and dynamic light scattering measurements we have determined the molecular weight M_w, radius of gyration R_G, and hydrodynamic radius R_H of the polymers. From these data we calculate a persistence length l_p for each polymer and find that increasing the size of the side chain increases l_p of the PPV backbone. Excitation profiles of the three polymers in solution show non-radiative decay of the photoluminescence at energies greater than ≈ 3 eV. Furthermore, the fraction of non-radiative decay is decreased as the intrinsic stiffness of the polymer is increased. Quantum efficiency determination of the polymers relative to quantum yield standard Rhodamine 6G in ethylene gylcol shows that increasing the persistence length of the polymer backbone increases the yield of the PPV system; for BCHA-PPV the quantum yield is 0.66 ± 0.05.

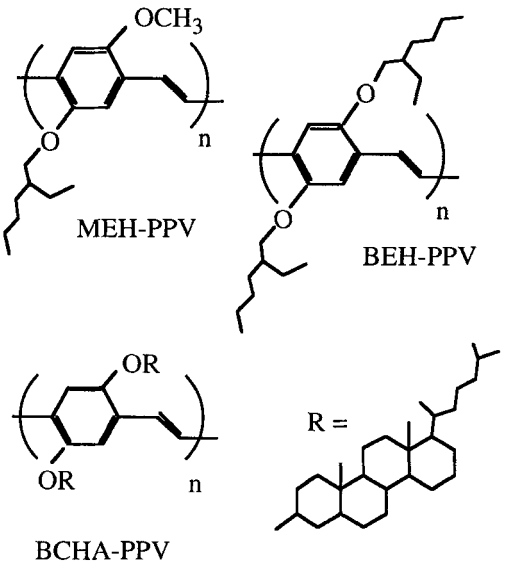

Figure 1: PPV derivatives

EXPERIMENTAL

PPV derivatives[10] were obtained from UNIAX corporation and HPLC p-xylene was obtained from Aldrich Chemical. Static light scattering measurements were performed using a Brookhaven Goniometer and a helium-neon laser (λ = 632.8 nm) light source. The weight average molecular weight M_w, and the radius of gyration R_G were determined in the limit $\theta \rightarrow 0$ and $c \rightarrow 0$ from the relation[11]

$$\frac{Kc}{R\Theta} = \frac{1}{M_w}\left(1 + \frac{q^2 R_G^2}{3}\right) + 2A_2 c \qquad (1)$$

where $K = 4\pi^2 n^2 (dn/dc)^2 / N_a \lambda_0$ and $q = (4\pi n/\lambda_0)\sin(\theta/2)$ is the scattering wavevector. In the above expressions R_θ is the excess Rayleigh ratio, c is the polymer concentration in g/ml, n is the index of refraction of the solvent, λ_0 is the wavelength of light, and dn/dc is the refractive index increment. Dynamic light scattering (DLS) measurements were performed in the Brookhaven

goniometer with an ALV-5000 correlator and a Coherent Krypton laser operating at a wavelength of 647.1 nm. Both wavelengths (647.1 nm and 632.8 nm) used in this experiment were chosen because none of the polymer samples absorbs light at these wavelengths.

The diffusion coefficient D for each of the polymers was obtained from the method of cumulants, which accounts for polydispersity of the samples. The hydrodynamic radius, R_H is calculated from the diffusion coefficient by the Stokes-Einstein equation, $D = kT/6\pi\eta_0 R_H$, where k is Boltzmann's constant, T is the temperature, and η_0 is the solvent viscosity[12].

Absorption spectra were recorded on an IBM Instruments 9420 UV-VIS spectrophotometer. Excitation and emission spectra were taken on an SLM Aminco 4800 spectrofluorometer. Samples were contained in 1 cm quartz cuvettes and data were collected at right angles from excitation beam. To minimize reabsorption and re-emission, polymer concentrations ($\approx 10^{-6}$ g/ml) were adjusted such that the optical density of all samples were less than 0.1 cm^{-1} at the highest absorption peak. The excitation profiles were normalized to a Rhodamine B quantum counter and the emission spectra were corrected for instrumental response.

Quantum yields were determined by comparing the total light emitted from the polymer solutions to the total light emitted from a known standard Rhodamine 6G dissolved in ethylene gylcol.

RESULTS AND DISCUSSION

Light Scattering

In Table 1 we summarize the data obtained from light scattering measurements. Intrinsic persistence lengths of the polymers were calculated with the Kratky-Perod model which treats a polymer as a gaussian distribution of statistical Kuhn lengths[13]. The radius of gyration, R_G is expressed as

$$R_G^2 = \frac{n_k b_k^2}{6} \tag{2}$$

where n_k is the number of Kuhn segments and b_k the length of the Kuhn segment. The persistence length, l_P is explicitly expressed by the relation

$$l_P = \frac{3R_G^2}{L} = \frac{3M_0 R_G}{M l_0} \tag{3}$$

where L is the contour length of the polymer, M_0 is the monomer molecular weight, l_0 is the monomer length, and M is the molecular weight of the polymer. We have estimated the length of a PPV monomer to be 0.6 nm. Using the values of R_G and M_W obtained from static light scattering, we find that the persistence length of the three polymers are BCHA-PPV 40 nm, BEH-

PPV 11 nm, and MEH-PPV 6 nm. Thus, the persistence length of the PPV backbone is increased by almost an order of magnitude with bulky side groups.

Table 1

	MEH-PPV	BEH-PPV	BCHA-PPV
M_W (g/mole	6.11 X 10^5	3.06 X 10^5	9.2 X 10^5
N monomers	2350	854	1055
R_G (nm)	52.4	42.1	92.1
R_H (nm)	35.9	19.8	33.7
$\rho = R_G/R_H$	1.46	2.13	2.73
lp (nm)	6.0	11.	40.

From our DLS measurements we obtained concentration independent hydrodynamic radii for all three polymers in the concentration range 10^{-4} g/ml, confirming that the polymers are in the dilute limit. These results are included in Table 1. We have calculated the parameter $\rho = R_G/R_H$ which also serves as a measure of the rigidity of a polymer. For flexible chains, ρ =1.5; more extended polymers have larger values[14]. The magnitude of ρ for the PPV derivatives scale from 1.46 for MEH-PPV to 2.76 for BCHA-PPV indicating that while MEH-PPV is a relatively compact coil, BCHA-PPV is a fairly expanded polymer.

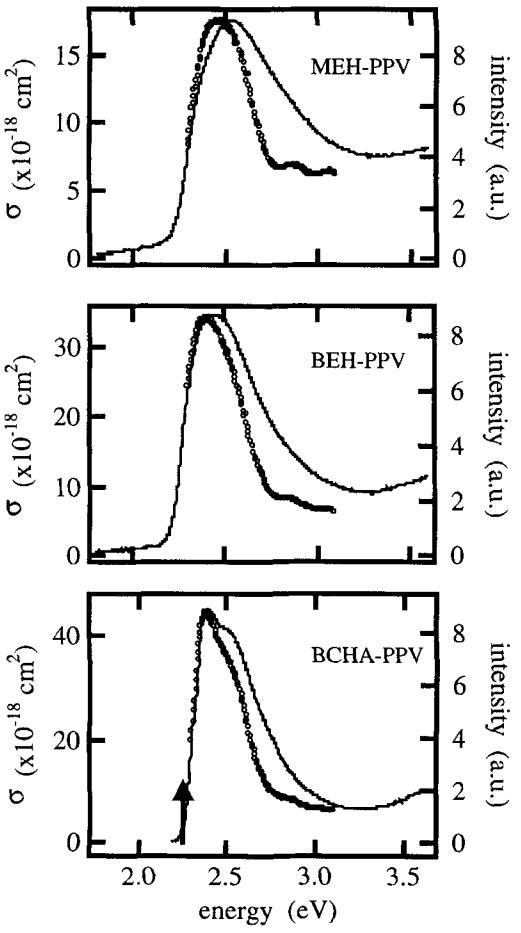

Figure 2: PPV derivative absorption (—) and excitation (○) profiles

Absorption and Excitation Spectroscopy

In figure 2 the absorption spectra of MEH-PPV, BEH-PPV, and BCHA-PPV in p-xylene are shown and compared to the excitation profiles measured at 550 nm. The absorption spectra of all three polymers display a flat region at low energies followed by the π - π^* electronic transition at $\approx$ 2.2 eV. While the absorption curves of the two flexible polymers, MEH-PPV and BEH-PPV display the characteristic broadened and featureless spectrum of conducting polymers in solution, the absorption spectra of the rigid BCHA-PPV

exhibits two peaks. The appearance of a second peak in the solution spectra of BCHA-PPV is attributed to an extended resolution of the underlying vibronic structure of the primary electronic transition. This increased resolution results from a more ordered structure[6]

When compared to the absorption spectra, the excitation profiles of the three polymers show a much larger absorbance relative to the excitation profiles at higher energies in MEH-PPV compared to BCHA-PPV. The reduction in the fraction of non-radiative decay for BCHA-PPV suggests that a more rigid, extended polymer backbone suppresses an important non-radiative decay mechanism.

Photoluminescence spectroscopy and Quantum Yields

In figure 3 photoemission spectra of MEH-PPV, BEH-PPV, and BCHA-PPV in p-xylene is shown with Rhodamine 6G in ethylene gylcol. Each of the polymers were excited on the low energy side of their absorption peaks. The emission spectra for all three polymers consist of a large electronic transition just below the excitation energy followed by vibronic progressions. Stokes shifts, determined from the difference in energy of the absorption and emission peaks, were found to decrease as the rigidity of the PPV backbone is increased. A similar reduction in Stokes shifts has been observed in systems with increased extension of the backbone[6]. Quantum yields were determined relative to a standard solution of Rhodamine 6G and calculated from the relation[15]

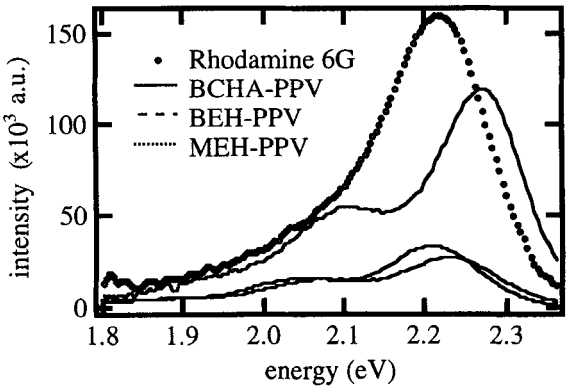

Figure 3: Photoemission spectra of PPV derivatives

$$Q_x = Q_r\left(\frac{A_r(\lambda_r)}{A_x(\lambda_x)}\right)\left(\frac{I_r(\lambda_r)}{I_x(\lambda_x)}\right)\left(\frac{n_x^2}{n_r^2}\right)\left(\frac{D_x}{D_r}\right). \quad (4)$$

In the above expression $A(\lambda)$ is the absorbance/cm of the solution at the exciting wavelength λ, $I(\lambda)$ is the intensity of the exciting wavelength λ, n is the index of refraction of the solution, and D is the integrated area under the emission spectrum. The subscripts r and x denote the reference sample and the unknown solution. The quantum yield for BCHA-PPV is 0.66 ± 0.05 compared to 0.20 ± 0.05 for MEH-PPV showing a strong correlation between intrinsic stiffness and radiative decay in PPV derivatives.

CONCLUSION

The combined results of absorption, excitation, and emission experiments show a strong correlation between a conjugated polymer's intrinsic stiffness and its optical properties. The correlation is observed in the appearance of vibronic structure in the absorption spectra, reduction in Stokes shifts, and an increase in quantum yield as the PPV backbone becomes more extended and is consistent with the picture of a more ordered structure. These results have also been observed for systems that have been macroscopically ordered through tensile drawing. Hagler *et. al.*[6] has interpreted the absorption of structurally ordered MEH-PPV as an interband transition with a series of vibrational sidebands. In these samples, the $0 \rightarrow 0$ transition dominates, with successive sidebands ($0 \rightarrow 1$, $0 \rightarrow 2$, etc.) having correspondingly smaller contributions as the number of optical phonons involved increases. Our results on the relatively well order BCHA-PPV indicate that absorption into the vibronic sidebands is associated with non-radiative decay at high pump energies. Because the excitation profiles of these polymers do not mirror the absorption spectra, emission intensities and resulting quantum yields are dependent upon the energy used to excite the electronic transition. The fact that the more rigid structure displays a lesser fraction of non-radiative decay is indicative of a suppression of an important non-radiative decay mechanism.

Acknowledgment: This research was partially funded by the National Science Foundation through NSF-DMR-9300366. CLG would like to thank Exxon for partial support.

REFERENCES

1. G. Gustafsson *et al.*, Nature 356, 47 (1992).
2. J.H. Burroughes *et al.*, Nature 347, 539 (1990).
3. D. Braun and A. Heeger, Appl. Phys. Lett. 58, 1982 (1991).
4. J. Aime, S. Ramakrishnan, R. Chance, and M. Kim, J. Phys. France 51, 963 (1990).
5. J. Bredas and A. Heeger, Macromolecules 23, 1150 (1990).
6. T.W. Hagler, K. Pakbaz, K.F. Voss, and A.J. Heeger, Phy. Rev. B 44, 865 (1991).
7. L. Smilowitz *et al.*, J. Chem. Phys. 98, 6504 (1993).
8. H. Bassler *et al.*, Syn. Metals 12, 49 (1992).
9. U. Rauscher, H. Bassler, D.D.C. Bradley, and M. Hennecke, Phy. Rev. B 42, 9830 (1990).
10. F. Wudl et al., *in Materials for Non-linear Optics: Chemical Perspectives* (American Chemical Society, Washington, D.C., 1991).
11. M. Huglin, Light Scattering from Polymer Solutions (Academic, New York, 1972).
12. B. Berne and R. Pecora, Dynamic Light Scattering with Applications to Chemistry, Biology, and Physics (John Wiley and Sons, New York, 1976).
13. O. Kratky and G. Porod, Recl. Trav. Chim. Pays-Bas 68, 1106 (1949).
14. H. Kromer *et al.*, Macromolecules 24, 1950 (1991).
15. J.N. Demas and G. Crosby, Journal of Physical Chemistry 75, 991 (1971).